SIMULATIONS OF BEAM LOADING COMPENSATION IN A WIDEBAND ACCELERATING CAVITY USING A CIRCUIT SIMULATOR INCLUDING A LLRF FEEDBACK CONTROL

Fumihiko Tamura*, Masanobu Yamamoto, Yasuyuki Sugiyama, Masahito Yoshii, Chihiro Ohmori,
Taihei Shimada, Masahiro Nomura, Katsushi Hasegawa, Keigo Hara, Masashi Furusawa
J-PARC Center, JAEA & KEK, Tokai-mura, Japan

Abstract

Magnetic alloy cavities are employed in the J-PARC RCS to generate high accelerating voltages. The cavity, which is driven by a vacuum tube amplifier, has a wideband frequency response and the beam loading in the cavity is multiharmonic. Therefore, the tube must generate a multiharmonic output current. An LTspice circuit model is developed to analyze the vacuum tube operation and the compensation of the multiharmonic beam loading. The model includes the cavity, tube amplifier, beam current, and LLRF feedback control. The feedback control consists of the I/Q demodulator including low pass filters, PI control, and I/Q modulator. In this article, we present the implementation of the LLRF functions in the LTspice simulations. The preliminary simulation results are also presented. The simulations fairly agree with the beam test results.

INTRODUCTION

Wideband magnetic alloy (MA) cavities [1] are employed in the rapid cycling synchrotron (RCS) of the Japan Proton Accelerator Research Complex (J-PARC) to generate high accelerating voltages. Because of the wideband frequency response [2], the multiharmonic beam loading must be compensated for high intensity beam acceleration. The MA cavity is driven by a vacuum tube amplifier, which outputs the multiharmonic compensation signal as well as the driving rf signal. The tube operation under heavy beam loading is not trivial.

To analyze the vacuum tube operation, we developed the LTspice [3] circuit models of the cavity, amplifier, and multiharmonic vector rf voltage control [4], which generates the compensation and driving rf signals.

In this article, the modeling of the digital circuits in the vector voltage control is described. The preliminary simulation results are compared with the beam test results.

CIRCUIT MODEL OF VECTOR RF VOLTAGE CONTROL

A simplified block diagram of the vector rf voltage control for a single harmonic is illustrated in Fig. 1. The digitized cavity gap voltage is fed to the I/Q demodulator, where the signal is multiplied by cosine and sine signals generated by the numerical controlled oscillators (NCO), and after the lowpass filter (LPF), the complex (I/Q) amplitude of

---
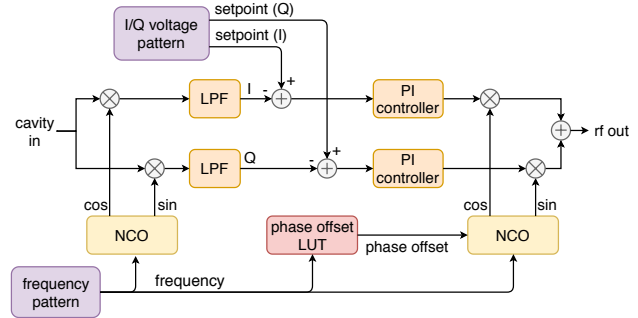
* fumihiko.tamura@j-parc.jp

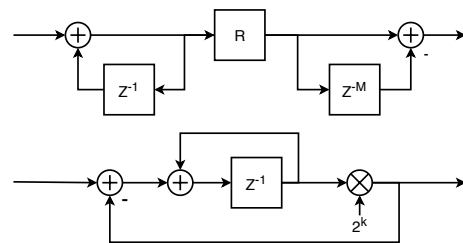Figure 1: Simplified block diagram of the vector rf voltage control.

Figure 2: Block diagrams of the digital lowpass filters. (Top) CIC filter and (bottom) leaky integrator.

the cavity gap voltage is obtained. It is compared with the I/Q setpoint and the proportional and integral (PI) controller block generates the compensation signal in the baseband. The output signal V_{out} is generated by the I/Q modulator as

$$V_{out} = I_{PI} \cos(h_n \omega_{rev} t + \phi') + Q_{PI} \sin(h_n \omega_{rev} t + \phi'), \quad (1)$$

where I_{PI} and Q_{PI} are the compensation signals from the PI controller, ω_{rev} is the revolutional angular frequency, and h_n the selected harmonic. With proper setting of the phase offset ϕ' between the I/Q demodulator and modulator, which is picked up from the lookup table (LUT) using the frequency signal for address of the LUT, the phase of the 1-turn transfer function satisfies the condition to close the feedback.

The response of the LPF determines the performance of the feedback. The CIC (cascaded integrator and comb) filter and the leaky integrator (LI) are implemented in the system. The block diagrams of the filters are shown in Fig. 2. The CIC filter consists of the integrator, resampler, and comb filter. The filter can be cascaded to obtain more attenuation in high frequency region. The transfer function of the CIC
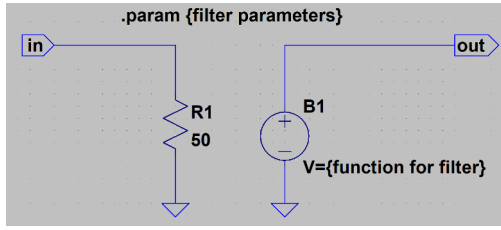
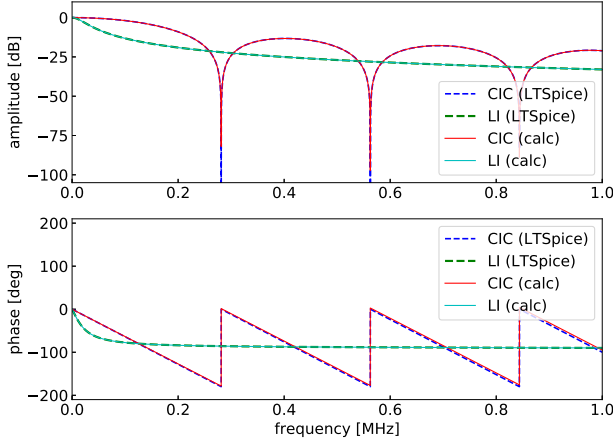Figure 3: Generic filter structure using the BV.

Figure 4: Comparisons of the amplitude and phase responses of the CIC filter and LI between the LTspice simulation and the calculation by using the transfer functions.

filter in the z-plane is

$$H_{\mathrm{CIC}}(z) = \left(\frac{1 - z^{-RM}}{1 - z^{-1}}\right)^N,\qquad (2)$$

where R is the decimation factor, M the number of the delay taps in the comb, and N the number of stages.

The generic filter structure using the behavioral voltage source (BV) in the LTspice is shown in Fig. 3. The BV is the voltage source of arbitrary functions. The single-stage CIC filter ($N = 1$) can be implemented simply by putting the expression of the BV as

```
V={CIC_gain/td_comb*(idt(V(CIC_in),0)
    -absdelay(idt(V(CIC_in),0),td_comb))}, (3)
```

where `CIC_gain` is the overall gain of the filter that is normally set to 1, and `td_comb` is the time delay in the comb part. `idt(x,0)` and `abs_delay(x,t)` are the LTspice functions for the integration along time and the time delay, respectively.

The transfer function of the LI is

$$H_{\mathrm{LI}}(z) = \frac{z^{-1}}{2^k + (1 - 2^k)z^{-1}},\qquad (4)$$

where 2^k is the coefficient shown in Fig. 2. Similar to the CIC filter, the LI can be implemented as

```
V={((2**k-1)*absdelay(V(LI_out),td_clk)
    +absdelay(V(LI_in),td_clk))/2**k}, (5)
```
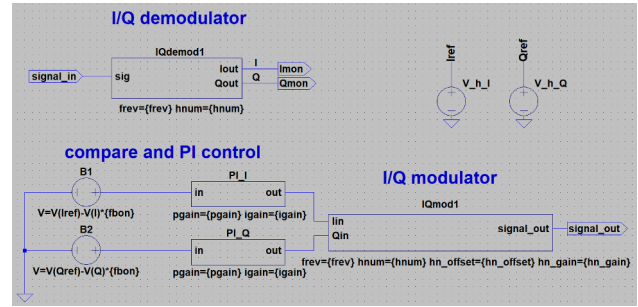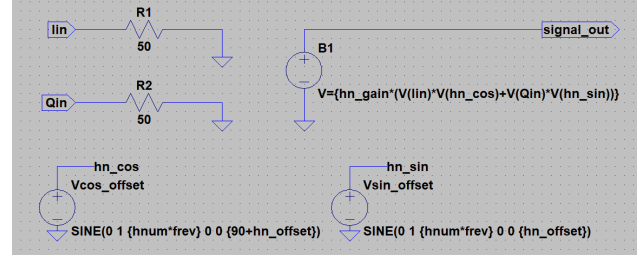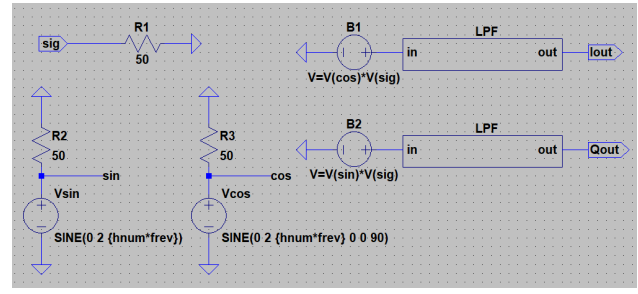
Figure 5: Circuit models of (top) the I/Q demodulator, (middle) the I/Q modulator, and (bottom) the complete feedback block.

where `td_clk` is the system clock period.

The frequency responses of the circuit models are obtained by the "AC analysis" in the LTspice, where the AC complex node voltages are computed as a function of frequency using a voltage source as the input signal. The simulated amplitude and phase responses of the single-stage CIC filter and the LI are compared with the transfer functions in Fig. 4. The parameters are `CIC_gain=1` and `td_comb=3.555` μs, which corresponds to 512 clock delays at the system clock frequency of 144 MHz for the CIC filter. For the LI, $k = 10$ and `td_clk=6.94` ns are used. The amplitude and phase responses of the LTspice simulations and the transfer functions perfectly agree.

The I/Q demodulator is implemented also by using the BV as shown in the top of Fig. 5. The cosine and sine signals at the frequency of selected harmonic (`hnum*frev`) are generated. The BVs multiply the input signal and the cosine and sine signals. The I/Q signals are obtained by applying the LPF. The PI controller can be implemented by using the generic filter structure with the function as

```
V={pgain*V(PI_in)+idt(igain*V(PI_in),0)}, (6)
```

where `pgain` and `igain` are the PI gains. The circuit model of the I/Q modulator is illustrated in the middle of
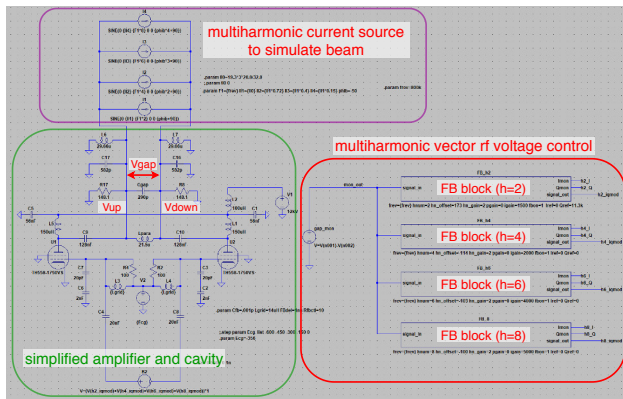
Figure 6: Complete circuit model including the multiharmonic vector voltage control, amplifier, and cavity.
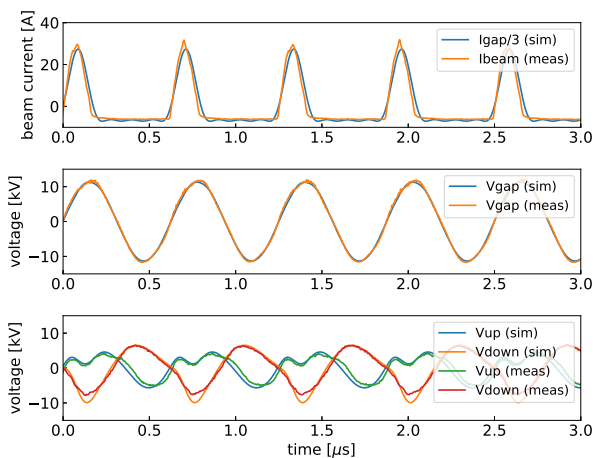

Figure 7: Comparisons of the simulated and measured waveforms of (top) beam current, (middle) gap voltage, and (bottom) voltages of the upstream and downstream gaps.

Fig. 5. The cosine and sine signals with a phase offset (`hn_offset`) are generated. The BV outputs the rf signal at the selected harmonic as Eq. (1).

Finally, the complete feedback block is composed as shown in the bottom of Fig. 5. Another BVs are used for comparison of the I/Q amplitude and the setpoint (`Iref`, `Qref`). Here, we note that the AC analysis of the feedback model does not work properly, because it contains two frequency domains, the rf frequency and the baseband. The transient analysis, which works fine, is still useful for investigating the vacuum tube operation.

SYSTEM LEVEL SIMULATION

Figure 6 shows the complete circuit model including the multiharmonic vector rf voltage control, amplifier, and cavity. The multiharmonic voltage control is realized by putting the feedback blocks for the selected harmonics ($h = 2, 4, 6, 8$). Since the harmonic number of the RCS is 2, the wake voltage contains the even harmonics only. Therefore the feedback blocks for the even harmonics are imple-

mented. The phase offsets in the feedback block are adjusted so that the feedback loops can be closed.

The MA cavity is modeled as a parallel LCR resonator. A single accelerating gap model is used for simplification, while the real cavity has three accelerating gaps. A tuning capacitor and a parallel inductor are connected at the accelerating gap to adjust the resonant frequency and Q value. The circuit constants are set so that the measured frequency response is reproduced. The amplifier has a push-pull configuration with two tetrode vacuum tubes (Thales TH558K), whose anodes are connected at the upstream and downstream of the accelerating gap via DC blocking capacitors. The anode voltage and screen grid voltage are set to 12 kV and 1.75 kV, respectively. The control grid (CG) is driven by the superposition of the DC voltage and the multiharmonic rf signal generated by the voltage control. The DC voltage of the CG is set to -356 V so that the idling anode current of each tube is 25 A.

The multiharmonic current source generates the current to simulate the beam current. The amplitude ratios are set based on the beam measurement. A factor of 3 is applied, because the single gap model is used to simulate the three gaps. The synchronous phase is realized by setting the phase offsets in the current sources.

For the simulation, the beam intensity is set to 5.2×10^{13} protons per pulse, which is equivalent to the beam power of 625 kW. At 10 ms from the injection, the synchronous phase is 40 deg and the gap voltage is 11.3 kV.

The simulated and measured beam current waveforms are compared in the top of Fig. 7, where the simulated waveform is divided by the factor of 3. One can see that using four harmonics is good enough to reproduce the beam current waveform. The gap voltage is regulated to the programmed voltage as plotted in the middle of Fig. 7. The higher harmonics of the wake voltage are well compensated and almost pure sinusoidal waveforms are observed. The simulated and measured waveforms nicely agree.

Since the amplifier generates the multiharmonic compensation signal, the voltage swings of the tubes are unbalanced. The voltage waveforms of the upstream and downstream of the accelerating gap, V_{up} and V_{down}, are plotted in the bottom of Fig. 7. The simulation reproduces the unbalanced tube operation fairly well. The shapes of V_{up} and V_{down} are quite similar for the simulation and measurement, while the maximum error of 35% is observed in the negative peak of V_{down}.

SUMMARY AND OUTLOOK

We newly developed the LTspice circuit models of the LLRF functions by using the behavioral voltage sources. The setup of the system level simulation is promising, where the preliminary simulation results agree with the measurement fairly well. The unbalanced tube operation due to the multiharmonic signal generation is a key issue for the high intensity acceleration. We will explore the possible countermeasures by using this simulation setup.

MC7: Accelerator Technology

T06 Room Temperature RF

REFERENCES

[1] C. Ohmori *et al.*, "High Field-Gradient Cavities Loaded with Magnetic Alloys for Synchrotrons", in *Proc. 18th Particle Accelerator Conf. (PAC'99)*, New York, NY, USA, Mar. 1999, paper THAL1, pp. 413–417.

[2] A. Schnase *et al.*, "MA Cavities for J-PARC with Controlled Q-value by External Inductor", in *Proc. 22nd Particle Accelerator Conf. (PAC'07)*, Albuquerque, NM, USA, Jun. 2007, paper WEPMN040, pp. 2131–2133.

[3] Analog Devices, LTspice, `https://www.analog.com/en/design-center/design-tools-and-calculators/ltspice-simulator.html`

[4] F. Tamura, Y. Sugiyama, and M. Yoshii "A prototype system of multiharmonic vector voltage control for the J-PARC rapid cycling synchrotron", presented at the LLRF 2017, Barcelona, Spain, Oct 2017, O-20.

This is a preprint — the final version is published with IOP